Research Square

Preprints are preliminary reports that have not undergone peer review.
They should not be considered conclusive, used to inform clinical practice,
or referenced by the media as validated information.

Adsorption–Thermal Regeneration of a Commercial Oxyfluorfen Formulation Using Organomodified Sepiolite: Equilibrium, Kinetics, and Cyclic Reuse

Ahed H. Zyoud

ahedzyoud@najah.edu

An-Najah National University

Raghad Tayeh

An-Najah National University

Shaher Zyoud

Palestine Technical University - Kadoorie

Ameed Amireh

An-Najah National University

A'laa Janem

An-Najah National University

Dongjun Cha

Korea Institute of Energy Research

Tae Woo Kim

Korea Institute of Energy Research

Wasim A. Zyoud

An-Najah National University

Research Article

Keywords: Sepiolite, Oxyfluorfen, OXYGAL, Emulsifiable concentrate, Aromatic petroleum hydrocarbons, Adsorption, Thermal regeneration, Reusability, Water treatment

Posted Date: November 23rd, 2026

DOI: https://doi.org/10.21203/rs.3.rs-11169717/v1

License: This work is licensed under a Creative Commons Attribution 4.0 International License.
Read Full License

Additional Declarations: No competing interests reported.

Adsorption–Thermal Regeneration of a Commercial Oxyfluorfen Formulation Using Organomodified Sepiolite: Equilibrium, Kinetics, and Cyclic Reuse

Abstract

A reusable adsorption–thermal-regeneration process was evaluated for treatment of the commercial oxyfluorfen emulsifiable concentrate OXYGAL using BAC-treated, heat-stabilized sepiolite. OXYGAL contains 240 g L^{-1} oxyfluorfen (OXY); for formulation-load estimates, the upper manufacturer-reported value of 600 g L^{-1} aromatic petroleum hydrocarbons (CAS No. 64742-94-5) was adopted, corresponding to an upper-bound solvent-to-active-ingredient ratio of 2.50 on a mass-per-volume basis. Batch adsorption and regeneration experiments were performed in triplicate with matched blank/recovery controls. Because single-wavelength UV–Vis analysis at 275.8 nm does not resolve OXY from co-formulants, the measured concentrations and adsorption capacities are reported as apparent nominal OXY-equivalent values. At 50 mg L^{-1} nominal OXY equivalent, 99.04% apparent removal was obtained after 40 min using 0.20 g adsorbent in 100 mL at pH 7 and 25 °C. Apparent removal remained above 99% at 20–50 mg L^{-1} and decreased to 68.86% at 150 mg L^{-1}. The linearized Langmuir model provided the better equilibrium fit (R^2 = 0.99218) with an apparent Q_0 of 45.09 mg g^{-1}, while the pseudo-second-order model gave the highest kinetic R^2 (0.99792); however, the pseudo-first-order model reproduced the reported experimental equilibrium uptake more closely. Increasing temperature from 15 to 55 °C reduced apparent removal from 99.50 to 32.00%, and an apparent activation energy of 30.38 kJ mol^{-1} was obtained. Thermal regeneration of the spent adsorbent at 500 °C for 1 h preserved most of the treatment performance, with apparent removal decreasing from 97% for fresh material to 91% after four regeneration cycles. The results support further development of thermally regenerable sepiolite for treatment of hydrophobic pesticide formulations, while chromatographic analysis remains necessary for component-specific quantification of OXY and formulation solvents.

Keywords: *Sepiolite; Oxyfluorfen; OXYGAL; Emulsifiable concentrate; Aromatic petroleum hydrocarbons; Adsorption; Thermal regeneration; Reusability; Water treatment*

1. Introduction

Pesticide formulations in agriculture could be transported to receiving water systems by means of runoff, drainage, spray drift, erosion, leaching, and improper disposal [1-4]. The difference is that

aqueous formulations include not only the active component but also solvents, surfactants, and other ingredients with different solubility, mobility, toxicity, and affinity to treatment solid phase. It is of special importance for the cases when treated water will be reused. In Palestine, the municipal treated wastewater is already used for irrigation of fields [5] whereas the treatment of streams of agro-industries, including olive mill wastewater, is still a significant issue [6]. Such treatment approaches should be developed in order to eliminate organic contaminants, reduce secondary wastes, and recycle the treatment solid phase.

Oxyfluorfen (OXY) is a diphenyl-ether herbicide with a mechanism of action targeting protoporphyrinogen oxidase [7, 8]. Very low aqueous solubility of the OXY (approximately 0.1 mg L^{-1}) and hydrophobic nature favor its sorption to soils, suspended solids, sediments, and organic phase [9, 10]. Therefore, the working media created from commercial emulsifiable concentrate with nominal OXY concentration tens of milligrams per liter could be considered as formulation-containing dispersions rather than solutions of OXY.

Adsorption is attractive for pesticide-contaminated water because of its operational simplicity and effectiveness under relatively mild conditions [11-16]. Its main limitation is that contaminants are transferred from the aqueous phase to a solid adsorbent that subsequently requires regeneration or disposal. Chemical or solvent regeneration can restore adsorption capacity but may generate a concentrated secondary liquid stream. Thermally stable inorganic adsorbents provide an alternative route in which retained organic matter can be removed or decomposed by heating while the mineral adsorbent is recovered for reuse.

Adsorption coupled with thermal regeneration has been used previously in our work on tetracycline, phenazopyridine, methyl orange, several organic contaminants, nitrate, and montmorillonite/sand composite [17-23]. This study extends our previous adsorption platform to a commercial herbicide formulation and a recently reported adsorbent. It evaluates adsorption performance alongside thermal stability, and reusability [24-28].

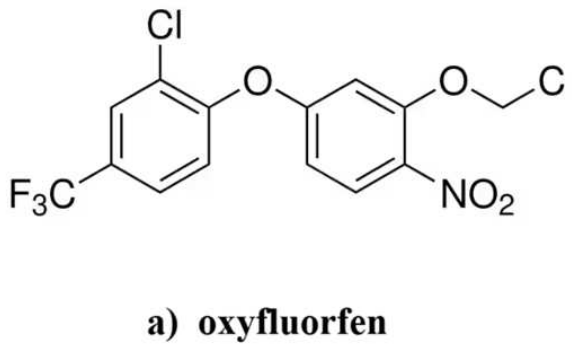
The procedure used in this study for the preparation of sepiolite has been described later on where the sepiolite was treated with benzalkonium chloride (BAC), washed, dried at 100 °C, and then calcined at 700 °C. Since the organic modifier has been subjected to this heat treatment step, the prepared sepiolite is referred to as the BAC-treated and heat-stabilized sepiolite.

The commercially available material was OXYGAL 240 EC (Tapazol Chemical Works Ltd.), obtained from a local agriculture distributor in Palestine. OXYGAL contains 240 g L^{-1} OXY (24% w/v; CAS No. 42874-03-3) and a major aromatic petroleum hydrocarbon fraction (CAS No. 64742-94-5). For quantitative co-load estimates in this manuscript, the upper manufacturer-reported value of 600 g L^{-1} was adopted. Thus, each nominal 1 mg L^{-1} of OXY introduced with

the product corresponds to an estimated 2.50 mg L^{-1} of aromatic petroleum hydrocarbons, before accounting for other formulation auxiliaries. The SDS also identifies C10 aromatic hydrocarbons, 1-methylpyrrolidin-2-one, branched ethoxylated 4-nonylphenol, and C10–C13 alkyl calcium benzenesulfonate.

Because several formulation constituents may contribute to absorbance in the UV region, the single-wavelength measurement used here cannot provide compound-specific OXY concentrations. Accordingly, the term apparent removal is used throughout this manuscript to denote the decrease in the calibrated UV-active formulation response expressed on the nominal OXY-equivalent scale. The estimated aromatic hydrocarbon values describe only the initial co-load introduced with OXYGAL and are not measurements of residual solvent concentration.

The objective of this study was therefore to evaluate BAC-treated, heat-stabilized sepiolite for removal of the UV-active fraction of a commercial oxyfluorfen EC formulation and to determine whether adsorption performance could be restored by thermal regeneration. The effects of contact time, formulation loading, adsorbent dosage, pH, and temperature were examined together with equilibrium and kinetic modeling, surface characterization, apparent activation-energy analysis, and four adsorption–regeneration cycles. The work provides a formulation-level assessment that is more representative of a commercial pesticide product than a pure-compound solution, while explicitly defining the analytical limits of the UV–Vis method.



a) oxyfluorfen

OXYGAL 240 EC

Tapazol Chemical Works Ltd.

Oxyfluorfen: 240 g L^{-1} (24% w/v)

Aromatic petroleum hydrocarbons:
CAS 64742-94-5; 600 g L^{-1}

Other SDS-listed auxiliaries:
C10 aromatic hydrocarbons; 1-methylpyrrolidin-2-one;
branched ethoxylated 4-nonylphenol;
C10–C13 alkyl calcium benzenesulfonate.

CAS 64742-94-5 is a mixture; no single molecular structure applies.

Figure 1. Molecular structure of oxyfluorfen and documented composition of the OXYGAL 240 EC formulation used in this study.

2. Experimental

2.1 Chemicals and materials

Sepiolite and benzalkonium chloride (BAC) were obtained from Sigma-Aldrich (St. Louis, MO, USA). Oxyfluorfen analytical standard (PESTANAL®, ≥98.0%) was obtained from Supelco/Sigma-Aldrich. Hydrochloric acid and sodium hydroxide (CS Chemical Company) were used for pH adjustment, and distilled water was used throughout. Adsorption working media were

prepared from OXYGAL 240 EC (Tapazol Chemical Works Ltd.), purchased from a local agricultural supplier in Palestine. The formulation contains 240 g L^{-1} OXY (24% w/v; CAS No. 42874-03-3). For the present calculations, the aromatic petroleum hydrocarbon solvent fraction (CAS No. 64742-94-5) was taken as 600 g L^{-1}, together with the additional SDS-listed auxiliaries described above. The batch/lot number was not recorded at the time of purchase.

2.2 Equipment

Residual formulation response was measured with a Shimadzu UV-1800 UV–visible spectrophotometer. Batch experiments were performed in a Labtech LSB-0 water-bath shaker, and solid–liquid separation was carried out using a LABTRON LLS-A12 centrifuge. Thermal treatment was performed in an MRC muffle furnace. Thermogravimetric behavior was measured using a SANAF thermal analyzer. X-ray diffraction (XRD) and scanning electron microscopy coupled with energy-dispersive X-ray spectroscopy (SEM–EDS) were used to examine crystal structure, morphology, and elemental composition; these analyses were performed in South Korea. FT-IR and TGA measurements were performed at An-Najah National University, Palestine.

2.3 Point of zero charge

The point of zero charge (pH_pzc) was determined by the pH-drift method. A 0.01 M NaCl solution was prepared, and six 50 mL portions were adjusted to initial pH values of 2, 4, 6, 8, 10, and 12 using 0.10 M HCl or 0.10 M NaOH. Treated sepiolite (0.10 g) was added to each bottle, and the suspensions were shaken at 150 rpm for 24 h at 25 ± 2 °C. After separation, final pH values were measured and $\Delta pH = pH_{final} - pH_{initial}$ was plotted against initial pH. The pH_pzc was taken at $\Delta pH = 0$, following the same general approach used in related clay-adsorption studies [22, 23].

2.4 Preparation of BAC-treated, heat-stabilized sepiolite

Pristine sepiolite was dispersed in distilled water and stirred for 2 h, followed by washing with distilled water to remove water-soluble impurities. The washed solid was dried at 100 °C and subsequently calcined at 700 °C. After cooling naturally to room temperature, the heat-treated sepiolite was modified with benzyldimethyltetradecylammonium chloride dihydrate, a C14 benzalkonium compound, using a dry-blending procedure adapted from Tang et al. [29]. A modifier loading of 10 wt% relative to the final sepiolite–modifier mixture was used. Accordingly, 0.90 g of calcined sepiolite and 0.10 g of the C14 benzalkonium modifier were combined with metal balls and mixed in an IKA Ultra-TURRAX Tube Drive at 6000 rpm for 10 min. The

resulting organomodified sepiolite was transferred to an airtight container and stored at room temperature until use.

2.5 Preparation and analytical basis of the OXYGAL working medium

An approximately 1.0 g L^{-1} nominal OXY stock was prepared by adding 2.0 mL of the commercial OXYGAL formulation to a 500 mL volumetric flask and diluting to volume with distilled water. Based on the verified OXYGAL content of 240 g L^{-1} OXY, this preparation corresponds to 0.96 g L^{-1} nominal OXY and is therefore appropriately described as an approximately 1.0 g L^{-1} stock. Operational media were prepared at nominal OXY-equivalent concentrations of 20, 30, 40, 50, 70, 90, 120, and 150 mg L^{-1}. The UV–Vis response was calibrated on a nominal OXY-equivalent basis using calibration standards corresponding to 10, 20, and 30 mg L^{-1}, selected within the linear response range of the instrument. Absorbance was measured at 275.8 nm, giving $A = 0.0455C + 0.265$ ($R^2 = 1.000$), where C is the formulation-derived nominal OXY-equivalent concentration. Based on the adopted formulation values, the estimated initial aromatic petroleum hydrocarbon co-load was calculated as $C_{arom} = (600/240)C_{OXY} = 2.50C_{OXY}$; thus, 50 mg L^{-1} nominal OXY corresponds to an estimated initial aromatic hydrocarbon co-load of 125 mg L^{-1}. Because the UV measurement is not component selective, calculated concentrations and adsorption capacities are reported as apparent nominal OXY-equivalent values. Component-specific confirmation would require HPLC or LC–MS for OXY and GC-based analysis for the aromatic solvent fraction.

2.6 Batch adsorption experiments and quality control

Batch adsorption experiments were conducted in 100 mL polyethylene vessels containing 100 mL of formulation-derived working medium. Unless otherwise specified, 0.20 g of treated sepiolite was used at 150 rpm and 25 °C for 40 min. Initial nominal OXY-equivalent concentration, adsorbent dosage, solution pH, contact time, and temperature were varied in separate experimental series. In the concentration, dosage, pH, and temperature studies, aliquots were collected at 5 min intervals during the 40 min contact period, centrifuged at 4000 rpm for 3 min, and the clear supernatant was measured at 275.8 nm using a Shimadzu UV-1800 spectrophotometer. Adsorption and regeneration studies were carried out in triplicate under identical conditions; the values cited are means of three determinations, with standard deviations provided as error bars where available. Blank/recovery pairs were also measured to evaluate losses that may occur due to volatilization, wall adsorption, formulation phase separation, and centrifugation processes.

Apparent removal (%) was calculated as $[(C_0 - C_e)/C_0] \times 100$, while apparent equilibrium uptake was determined as $q_e = (C_0 - C_e)V/m$, where C_0 and C_e are concentrations determined based on

the same nominal OXY-equivalent calibration curve derived from the formulation, V is the volume of the medium, and m is the weight of adsorbent used. Apparent removal and uptake refer to changes in the UV-activity of formulation caused by the specified handling process and do not correspond to any independent determination of the adsorbed amount of OXY or solvent. The estimated aromatic hydrocarbon loading, $C_{arom} = 2.50C_{OXY}$, refers only to the initial amount of aromatic compound introduced with OXYGAL.

Table 1. *Experimental conditions used to evaluate the main operational parameters in batch adsorption.*

Parameter	Experimental range/condition	Selected condition
Initial nominal OXY-equivalent concentration	20, 30, 40, 50, 70, 90, 120, 150 mg L^{-1}	50 mg L^{-1}
Adsorbent dosage	0.20–0.60 g per 100 mL	0.20 g
pH	2.19, 2.49, 3.24, 4.24, 7.00, 9.85	7.00
Contact time	0–40 min	40 min
Temperature	15, 25, 35, 45, 55 °C	25 °C
Agitation rate	150 rpm	150 rpm
Solution volume	100 mL	100 mL
Estimated aromatic petroleum hydrocarbons (600 g L^{-1} basis)	50, 75, 100, 125, 175, 225, 300, 375 mg L^{-1}	125 mg L^{-1}

2.7 Equilibrium, kinetic, and apparent activation-energy analysis

The equilibrium data were analyzed on the basis of the Langmuir isotherm $q_e = Q_0K_LC_e/(1 + K_LC_e)$ and Freundlich isotherm $q_e = K_FC_e^{(1/n)}$. The series of isotherms was performed for nominal OXY-equivalent concentrations of 20, 30, 40, 50, 70, 90, 120, and 150 mg L^{-1} at pH 7, 25 °C, 150 rpm, 0.20 g of adsorbent, 100 mL of solution, and 40 min of contact time. Kinetics of the adsorption process were examined at a concentration of 50 mg L^{-1} of nominal OXY equivalent for 0.20 g of adsorbent in 100 mL at pH 7, 25 °C, 150 rpm, and 40 min according to the linearized pseudo-first-order (PFO), pseudo-second-order (PSO), and intraparticle-diffusion models. Due to different transformations in linearized forms of the isotherms, R^2 values were considered along with the comparison of experimental and calculated q_e values [30-32].

2.8 Thermal regeneration and reuse

Thermogravimetric analysis was used to assess the temperature region associated with thermal degradation before regeneration testing. Following adsorption, the formulation-loaded solid was

recovered, placed in a ceramic crucible, and thermally regenerated in an MRC muffle furnace at 500 °C for 1 h, The regenerated material was cooled naturally to room temperature and reused under the selected adsorption conditions: 0.20 g adsorbent, 100 mL working medium containing 50 mg L^{-1} nominal OXY equivalent, pH 7, 25 °C, 150 rpm, and 40 min contact time. Four successive adsorption–regeneration cycles were performed. The 500 °C regeneration treatment is distinct from the 700 °C calcination used during initial adsorbent preparation.

3. Results and discussion

3.1 Characterization of BAC-treated, heat-stabilized sepiolite

X-ray diffraction revealed that the major reflections of the sepiolite mineral phase were still present after treatment, confirming that the primary inorganic structure was retained. The SEM photographs showed the typical fibrous/needle structure of the sepiolite. After treatment, the fibers were seen to be more woven together. EDS spectra were made up primarily of O, Si, and Mg, with other elements of mineral content being present in small amounts. Thus, the combined information suggests that the treatment changed the texture but not the specific inorganic framework of sepiolite needed for adsorption and heating.

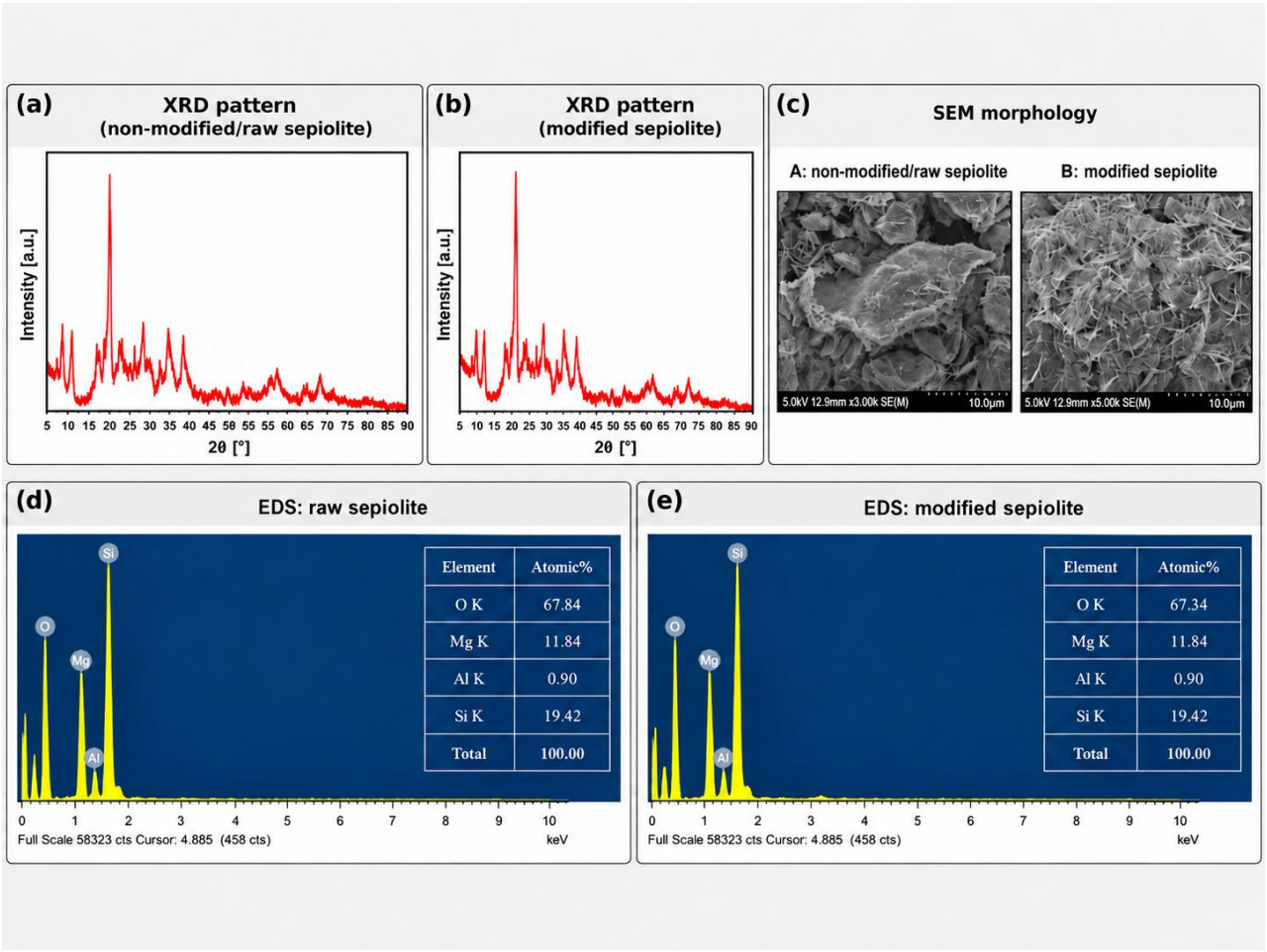


Figure 2. Characterization of sepiolite: (a) XRD pattern of the non-treated and treated material; (b) SEM images of raw sepiolite and treated sepiolite, with a 10 μm scale bar; and (c,d) representative EDS spectra of raw and treated sepiolite.

The pH_pzc of the material after treatment was estimated to be around 8.9. Since the adsorption pH is set at 7, then it is expected that the charge on the surface would be more positive as compared to those at higher pH values. However, the commercial product is composed of hydrophobic organic components, surfactants, and dispersed phases; thus, the pH dependency cannot be explained electrostatically.

The calibration for the UV–Vis method was made from nominal concentrations of 10, 20, and 30 mg/L of OXY-equivalents and the calibration was linear in this range ($R^2 = 1.000$). Therefore, it is justified to determine the nominal OXY-equivalent concentrations using absorbance, but the lack of selectivity in wavelength indicates that the measurement is of the entire formulation response and not of OXY itself.

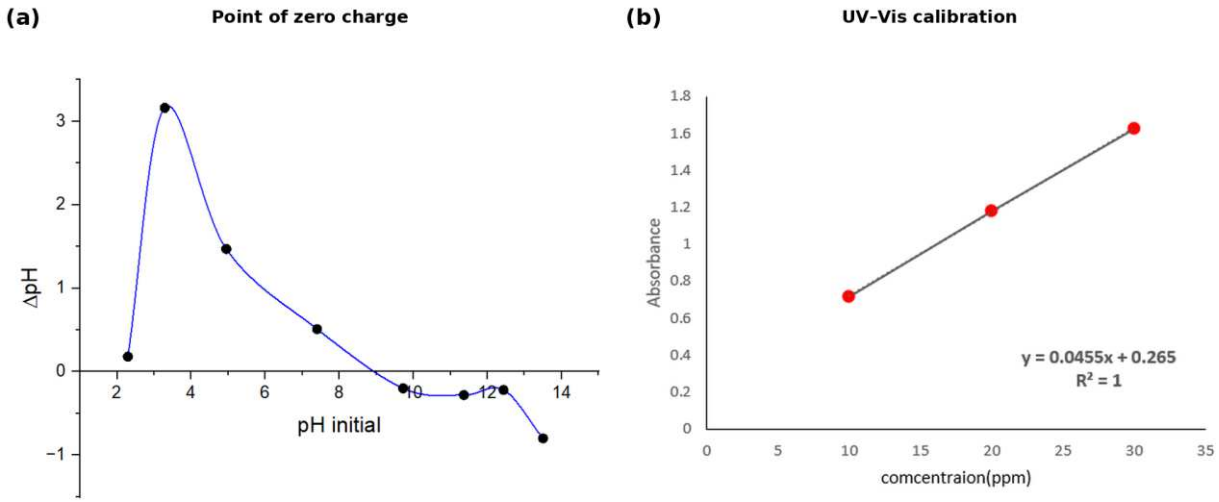


Figure 3. (a) Determination of the point of zero charge of treated sepiolite and (b) UV–Vis calibration at 275.8 nm using 10, 20, and 30 mg L^{-1} nominal OXY-equivalent standards from the experimental dataset.

3.2 Effect of operational parameters in batch adsorption

This group of operational parameters was taken collectively since it is what determines the batch treatment window in practice. Time profile indicated an initially fast drop in the apparent concentration, followed by a gradual approach to a plateau level. Samples were taken every 5 min and 40 min was chosen as the common comparison time for loading capacity, adsorbate dosage, pH and temperature.

Formulation loading had a profound effect on apparent removal. When the OXY-equivalent concentration was nominally at 20, 30, 40, and 50 mg L^{-1}, apparent removal was 99.40, 99.30,

99.18, and 99.04%, respectively. When the loading was increased to 70, 90, 120, and 150 mg L^{-1}, removal was reduced to 95.93, 91.22, 86.83, and 68.86%. This indicates an estimated load range for aromatic hydrocarbons of 50-375 mg L^{-1} based on the chosen formulation concentration of 600 g L^{-1}.

The increase in the adsorbent dose led to a reduction in the remaining UV active response, which is due to a higher amount of available surface for the adsorption process. But 0.20 g per 100 mL was already a large apparent removal and was therefore chosen as the dosage for the experiment. The solution pH showed an influence on the performance of the treatment process. The best apparent removal was found at around pH 7, whereas there were worse results at lower and higher pH levels, especially at pH 9.85. This is probably due to the fact that the pH_pzc value is 8.9; however, since a multicomponent emulsion is used, there is also hydrophobic partitioning and surfactants involved in the system.

Temperature produced the largest change in apparent removal among the operational variables examined. Apparent removal was 99.50% at 15 °C and 99.04% at 25 °C, but decreased to 84.00, 60.00, and 32.00% at 35, 45, and 55 °C, respectively. The trend is consistent with weaker net retention of formulation-derived UV-active constituents at higher temperature, although changes in emulsion stability and partitioning may also contribute.

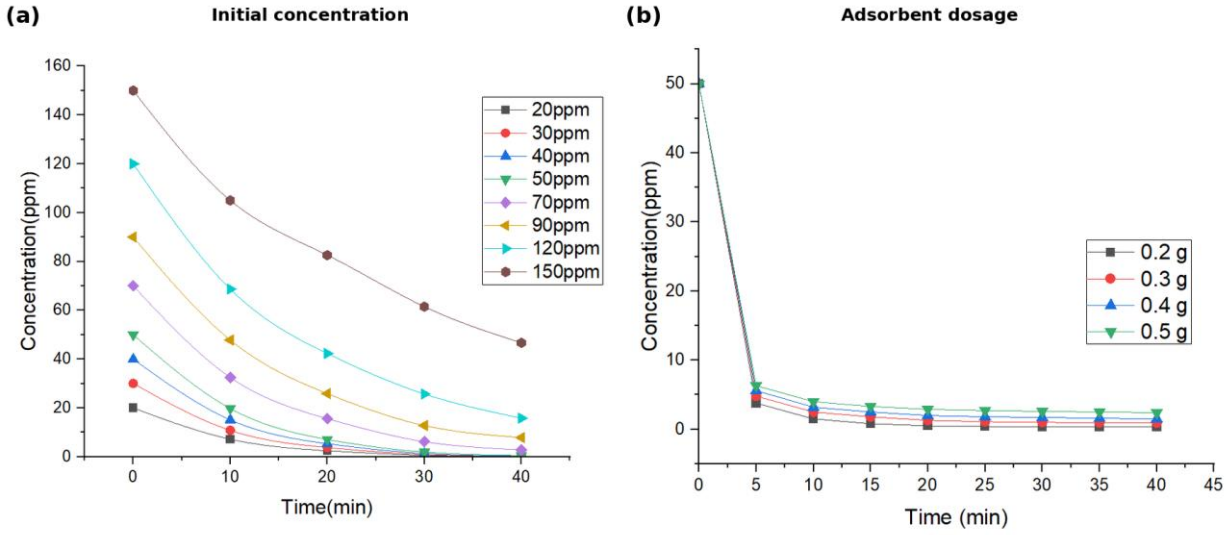


Figure 4. Effect of operational parameters under batch conditions: (a) initial nominal OXY-equivalent concentration and (b) adsorbent dosage. Curves show formulation-derived apparent concentrations from triplicate experiments.

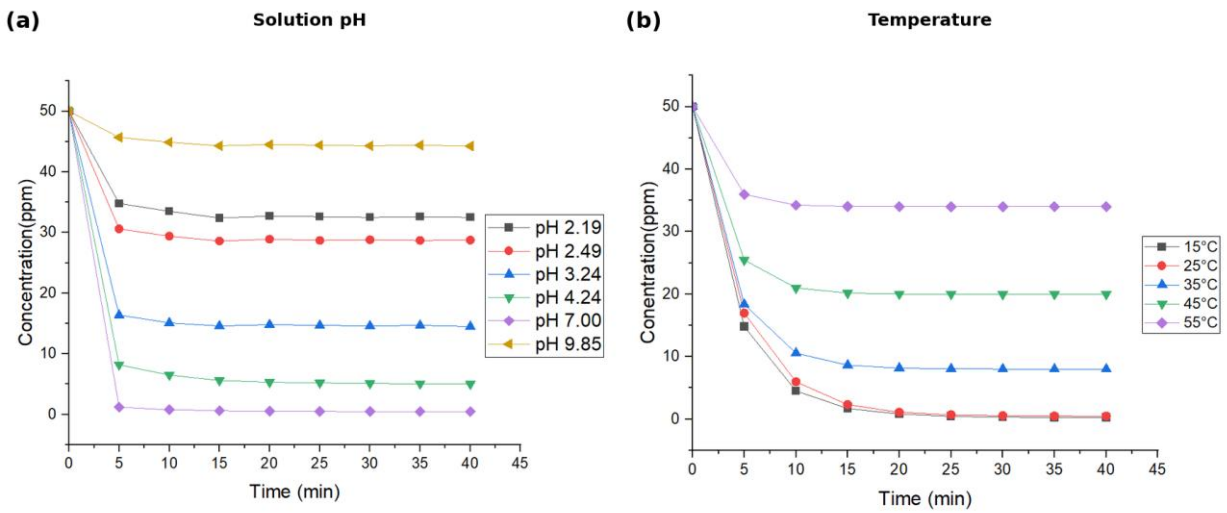


Figure 5. Effect of operational parameters under batch conditions: (a) solution pH and (b) temperature. Apparent concentration was monitored at 275.8 nm.

Table 2. Effect of initial nominal OXY-equivalent concentration on removal efficiency and the corresponding estimated aromatic petroleum hydrocarbon co-load calculated using the 600/240 = 2.50 composition ratio.

Nominal OXY-equivalent (mg L^{-1})	Estimated aromatic petroleum hydrocarbons (mg L^{-1})	Removal (%)
20	50	99.40
30	75	99.30
40	100	99.18
50	125	99.04
70	175	95.93
90	225	91.22
120	300	86.83
150	375	68.86

3.3 Adsorption equilibrium

The linearized Langmuir model yielded Q_0 = 45.09 mg g^{-1} and K_L = 0.4563 L mg^{-1} with R^2 = 0.99218. The Freundlich model gave K_F = 17.97, 1/n = 0.23678, and R^2 = 0.94184. Thus, among the two tested linearized representations, Langmuir described the apparent equilibrium dataset more closely. The Freundlich value 1/n < 1 is also consistent with favorable uptake within that empirical model. These parameters describe the formulation-derived UV response on the nominal OXY-equivalent calibration basis and should not be interpreted as compound-specific OXY constants.

The fitted Q_0 should be interpreted as an apparent regression-derived capacity rather than a strict physical saturation limit. The highest-loading experimental point is slightly above the fitted Langmuir asymptote under the common batch conditions, indicating sensitivity of the linearized

fit to experimental scatter and to the multicomponent formulation matrix. Accordingly, Q_0 is used here to characterize the reported equilibrium dataset and not to rank the present material directly against adsorption capacities obtained for pure individual compounds.

Table 3. Langmuir and Freundlich parameters on the apparent nominal OXY-equivalent calibration basis used in the original dataset.

Model	Parameter	Apparent nominal OXY-equivalent value	Interpretation
Langmuir	Q_0 (mg g^{-1})	45.09	Apparent capacity from formulation-based UV calibration
	K_L (L mg^{-1})	0.4563	Fitted Langmuir affinity constant
	R^2	0.99218	Model correlation coefficient
Freundlich	K_F	17.97	Apparent Freundlich coefficient
	1/n	0.23678	Favorable adsorption (1/n < 1)
	R^2	0.94184	Model correlation coefficient

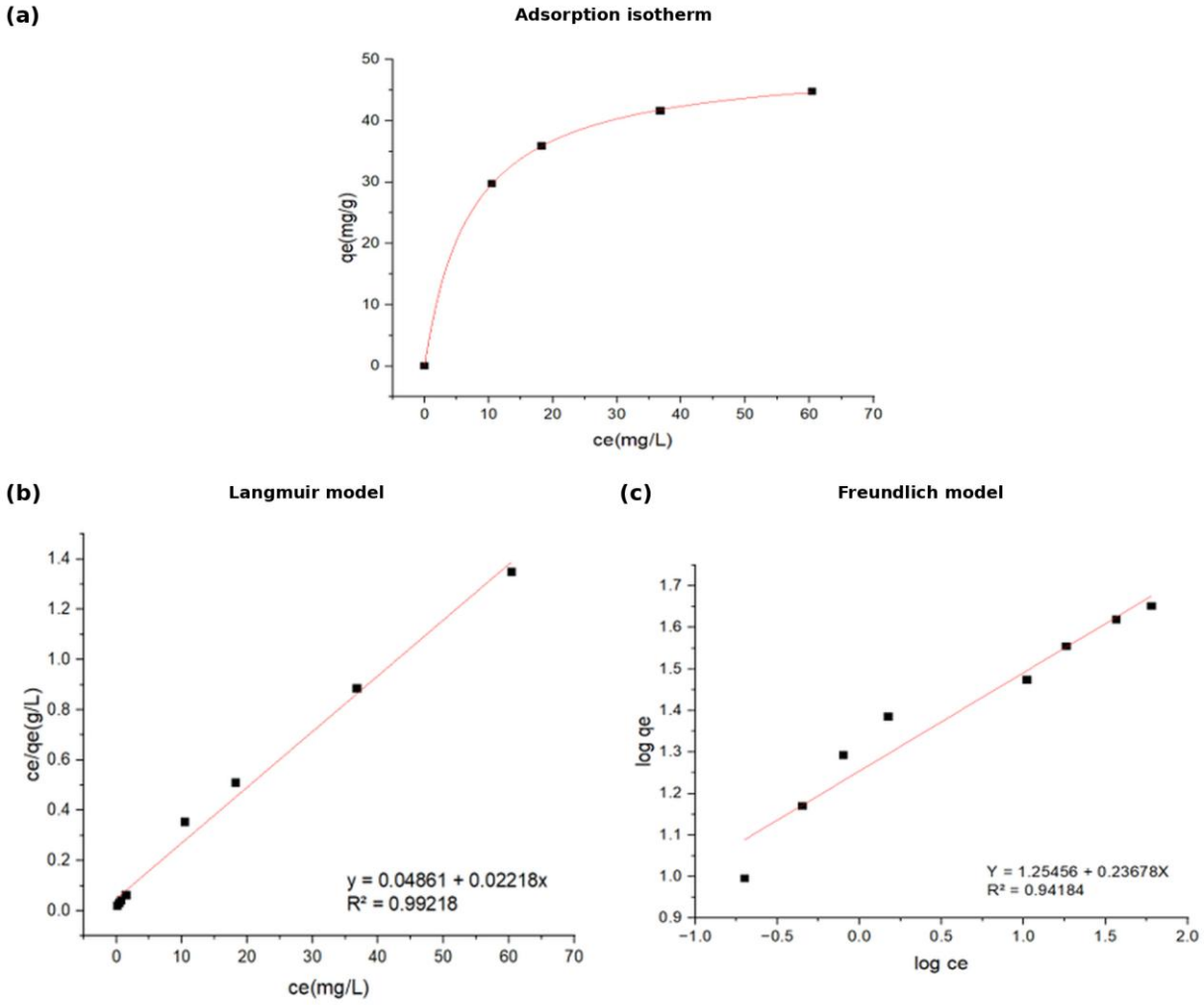


Figure 6. Equilibrium analysis on the apparent nominal OXY-equivalent basis: (a) adsorption isotherm, (b) Langmuir representation, and (c) Freundlich representation.

3.4 Adsorption kinetics

Kinetic models provided a consistent trend of fast initial sorption, followed by a slower approach towards the ultimate equilibrium concentration. Based on the PFO kinetic model, q_e = 23.48 mg g^{-1} was found, which is close to the experimentally found value 23.20 mg g^{-1} (R^2 = 0.99222). As for the PSO kinetic model, it produced the largest value of R^2 (0.99792), but overestimated q_e (31.27 mg g^{-1}). Thus, PSO provides the highest linearized R^2, while PFO better mimics the experimentally measured equilibrium value. It is important to stress that the presence of high PSO R^2 does not necessarily mean chemisorption [31, 32].

Intraparticle diffusion provided k_p = 3.73138 mg g^{-1} $min^{-½}$, B = 0.61214 mg g^{-1} and R^2 = 0.99282. Since the intercept is positive, it means that the regression line does not pass through the origin, which suggests that intraparticle diffusion is not the only rate-controlling step. Other factors may affect the time dependence such as film transfer, boundary layer effect, adsorption onto accessible sites, intra-fiber diffusion and dispersion process of formulations.

Table 4. Kinetic parameters on the apparent nominal OXY-equivalent calibration basis used in the original dataset.

Model	Parameter	Apparent nominal OXY-equivalent value	Interpretation
Pseudo-first-order	q_e,exp (mg g^{-1})	23.20	Experimental apparent uptake
	k_1 (min^{-1})	0.0809	PFO rate constant
	q_e,calc (mg g^{-1})	23.48	Calculated apparent uptake
	R^2	0.99222	Model correlation coefficient
Pseudo-second-order	k_2 (g mg^{-1} min^{-1})	0.00226	PSO rate constant
	q_e,calc (mg g^{-1})	31.27	Calculated apparent uptake
	R^2	0.99792	Highest R^2 among tested kinetic models
Intraparticle diffusion	k_p (mg g^{-1} $min^{-½}$)	3.73138	Diffusion slope
	B (mg g^{-1})	0.61214	Positive intercept; diffusion not sole rate control
	R^2	0.99282	Model correlation coefficient

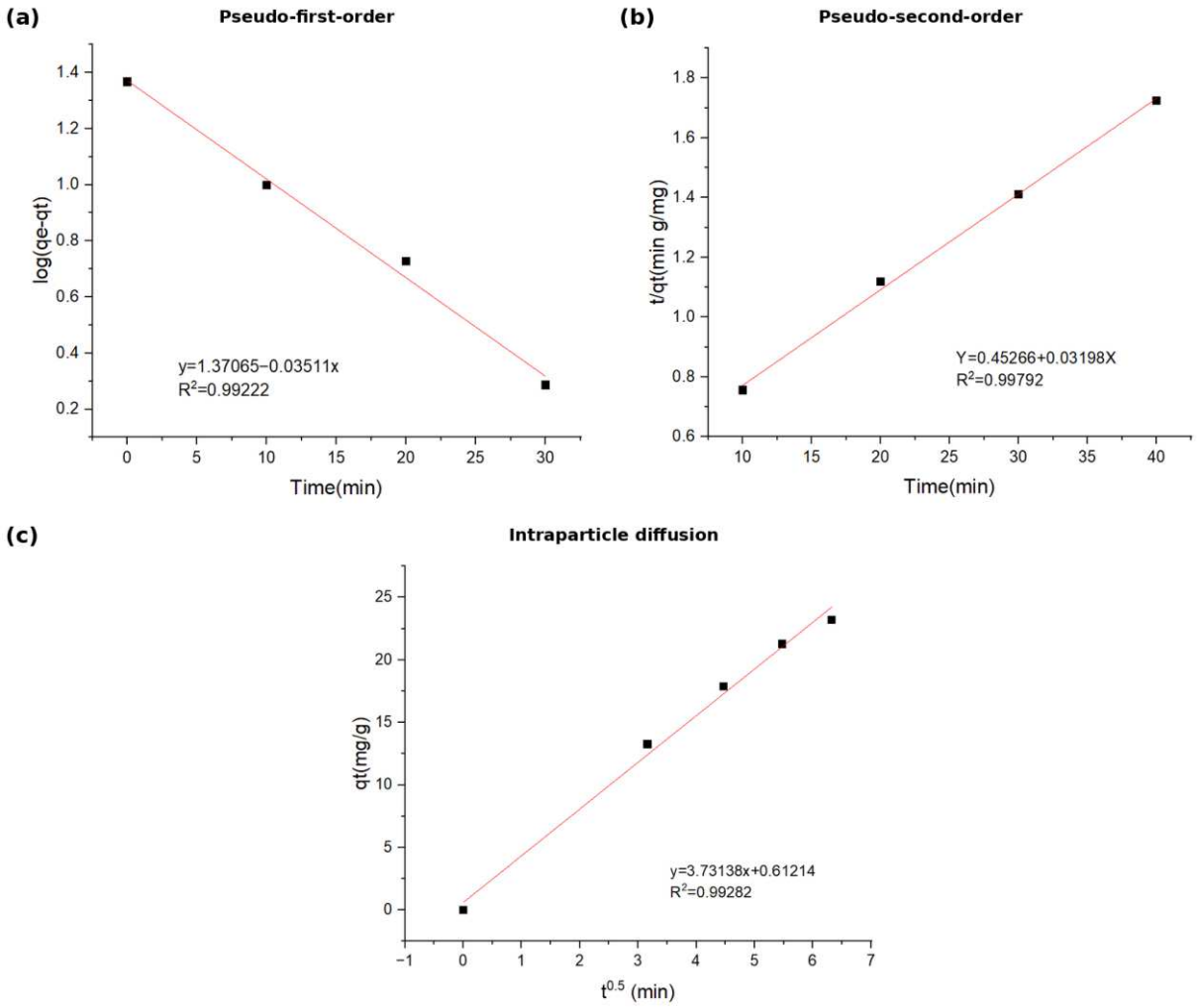


Figure 7. Linearized kinetic-model plots on the apparent nominal OXY-equivalent basis: (a) pseudo-first-order, (b) pseudo-second-order, and (c) intraparticle-diffusion model.

3.5 Temperature dependence, activation energy, and adsorption mechanism

Based on the Arrhenius equation, the activation energy was obtained as 30.38 kJ mol^{-1} (R^2 = 0.99920). Such a close value to 30.37 kJ mol^{-1} obtained before for the adsorption of phenazopyridine on calcined montmorillonite [22] does not mean the same adsorption mechanism. The rate constant which was used in the Arrhenius equation is not described enough in this case for identification of the specific elementary process and E_a is just considered as an apparent activation energy.

Taking into account the pH effects, structure of fibrous sepiolite, temperature effects, FT-IR variations, and kinetics, uptake seems to involve several mechanisms operating simultaneously, such as hydrophobic interaction, van der Waals forces, hydrogen bonds with hydroxyl/silanol surface groups, electrostatic effects, mass transfer, and diffusion in between fibers. Because OXYGAL also contains aromatic hydrocarbons and surfactant-type auxiliaries, partitioning among formulation components may additionally influence the observed response. Although

Tang et al. [29] showed that a 10 wt% C14 benzalkonium modification can produce organophilic sepiolite, their material was prepared by dry blending and was not subjected to the aqueous washing and 700 °C calcination used here. Therefore, no specific BAC-mediated adsorption mechanism is proposed for the present calcined material.

3.6 FT-IR, thermal stability, regeneration, and reuse

FT-IR spectra of raw and treated sepiolite showed the characteristic OH/H_2O- and silicate-associated bands of the mineral framework. Pure OXY displayed characteristic organic absorptions, while the formulation-loaded adsorbent exhibited changes in several band positions and intensities after contact with the solid. These spectral changes are consistent with interaction of formulation-derived organic constituents with the sepiolite surface; however, overlap among OXY and co-formulant bands prevents unambiguous assignment of all features. No clear new band attributable to formation of a new covalent structure was observed, so the FT-IR data do not provide evidence for covalent bond formation during adsorption.

According to TGA results, the thermal stability of the treated mineral was sufficient for the selected regeneration temperature of 500 °C. During the cyclic experiment, apparent removal was 97% for fresh material and 96, 94, 92, and 91% for regeneration cycles 1–4, respectively. Thus, the fourth-cycle apparent removal corresponded to approximately 93.8% of the fresh-cycle value in the reuse series.

Heating at 500 °C is therefore supported as an effective regeneration treatment for restoring most of the measured adsorption performance. However, regeneration should be distinguished from confirmed mineralization. OXY contains Cl, F, and N, and the commercial formulation also contains aromatic hydrocarbons and other organic auxiliaries; TGA, FT-IR, and restored adsorption performance do not identify all gaseous, condensed, or solid thermal products. Off-gas and residue analysis would be required to establish complete destruction pathways and environmental emissions from the thermal step.

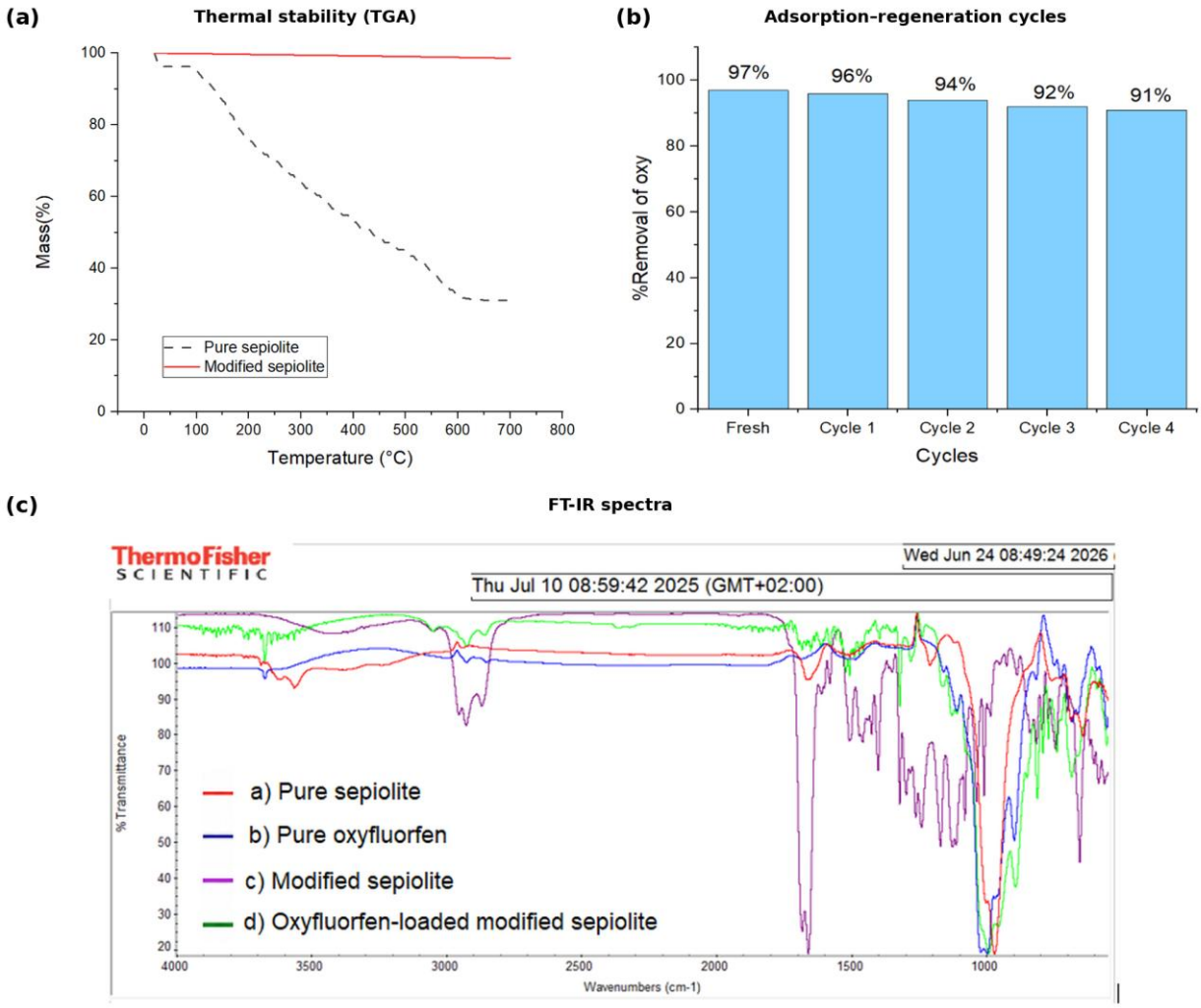


Figure 8. Thermal stability and regeneration behavior: (a) TGA profiles of raw and treated sepiolite; (b) apparent removal with fresh and regenerated adsorbent over four adsorption–regeneration cycles; and (c) FT-IR spectra of sepiolite, oxyfluorfen, treated sepiolite, and formulation-loaded treated sepiolite. Regeneration was performed at 500 °C for 1 h.

Table 5. Removal performance during repeated adsorption–regeneration experiments

Adsorption–regeneration stage	Removal (%)
Fresh	97
Cycle 1	96
Cycle 2	94
Cycle 3	92
Cycle 4	91

3.7 Comparison with related adsorption–thermal-regeneration systems

The present work extends a series of clay-based adsorption–thermal-regeneration studies [17-23]. Previous systems used regeneration temperatures of approximately 550–700 °C and generally maintained high removal over repeated reuse. In comparison, the present sepiolite system was regenerated at 500 °C for 1 h and retained 91% apparent removal after four cycles. The lower regeneration temperature is operationally encouraging, although direct performance ranking is not

appropriate because the earlier studies involved different pollutants, adsorbents, analytical endpoints, and solution conditions. Most importantly, the apparent capacity reported here is derived from a multicomponent commercial formulation and is not chemically equivalent to a pure-compound adsorption capacity.

Table 6. Comparison with related thermally regenerable clay systems.

Adsorbent	Pollutant/system	Reported capacity	Regeneration condition	Reuse performance	Ref.
Montmorillonite	Tetracycline	—	Thermal treatment	Multiple cycles	[17]
Modified natural clay	Tetracycline	85.54 mg g^{-1}	550 °C, 120 min	Five cycles	[18]
$ZnCl_2$-modified kaolinite	Methyl orange	—	600 °C	82–85% over five cycles	[19]
Modified natural clay	Phenazopyridine	36.01 mg g^{-1}	550 °C, 120 min	Regenerable	[20]
Thermally stable natural clay	Multiple organics/nitrate	—	600 °C	>85% through five cycles	[21]
Mnt/sand composite	Phenazopyridine	8.98 composite; 44.90 active Mnt	~550 °C	87–90%	[23]
Heat-treated montmorillonite	Phenazopyridine	61.53 mg g^{-1}	700 °C	>91%	[22]
Modified sepiolite (present study)	Commercial OXYGAL formulation	45.09 mg g^{-1} apparent OXY-equivalent; ≈157.82 mg g^{-1} known-organic formulation equivalent*	500 °C, 1 h	91% after cycle 4	This work

**The formulation-equivalent value was calculated from the quantified OXYGAL composition of 240 g L^{-1} OXY plus 600 g L^{-1} aromatic petroleum hydrocarbons, giving a factor of 3.50 relative to OXY. It is an estimated formulation-load equivalent and not a directly measured total-organic adsorption capacity. Other SDS-listed organic auxiliaries were not included because their concentrations were not quantitatively specified.*

3.8 Practical significance and study limitations

A practical strength of the study is that it evaluates a commercial pesticide formulation rather than an idealized pure-compound solution. At the selected nominal OXY loading of 50 mg L^{-1}, the adopted product composition corresponds to an estimated initial aromatic petroleum hydrocarbon co-load of approximately 125 mg L^{-1}, in addition to other formulation auxiliaries. Demonstrating high apparent removal under this mixed-organic loading and maintaining 91% performance after four thermal-regeneration cycles supports further development of sepiolite as a reusable treatment material.

The adsorption–thermal-regeneration strategy also avoids the use of a liquid solvent regenerant during the tested reuse step, potentially reducing secondary regeneration wastewater. At the same time, heating to 500 °C imposes an energy requirement and may generate volatile or partially oxidized products. Future process assessment should therefore quantify energy use per kilogram

of regenerated adsorbent and per volume of treated water, adsorbent mass recovery and attrition, furnace loading, heat recovery, and off-gas treatment.

The principal analytical limitation is the lack of component selectivity in the single-wavelength UV–Vis method. The reported percentages and capacities quantify apparent formulation-level response reduction and cannot separate OXY from aromatic petroleum hydrocarbons or other UV-active constituents. Future validation should combine HPLC or LC–MS for OXY with GC–MS or equivalent analysis for volatile/semi-volatile formulation components, and should extend the treatment to real agricultural drainage or wastewater matrices. The confirmed triplicate design and matched blank/recovery controls strengthen reproducibility, but reporting the underlying replicate values and control recoveries would further improve the final analytical validation. In addition, the exact BAC loading used during the original aqueous modification was not preserved in the thesis record; the 10 wt% value reported by Tang et al. [29] is therefore treated only as a literature benchmark rather than as a measured preparation parameter for the present adsorbent.

4. Conclusion

BAC-treated, heat-stabilized sepiolite effectively reduced the UV-active response of the commercial OXYGAL 240 EC formulation under the investigated batch conditions. At 50 mg L^{-1} nominal OXY equivalent, 99.04% apparent removal was obtained after 40 min using 0.20 g adsorbent per 100 mL at pH 7 and 25 °C. The concentration study showed >99% apparent removal at 20–50 mg L^{-1}, followed by a progressive decrease at higher formulation loading.

The equilibrium data were better described by the Langmuir model than by the Freundlich model, yielding an apparent maximum adsorption capacity (Q_0) of 45.09 mg g^{-1} on the formulation-derived nominal OXY-equivalent basis, corresponding to an estimated 157.82 mg g^{-1} when expressed on the basis of the quantified OXY plus aromatic petroleum hydrocarbon content of OXYGAL. Kinetic analysis showed that PSO produced the highest R^2, whereas PFO predicted the experimental equilibrium uptake more accurately, supporting a cautious, non-mechanistic interpretation of the linearized models. Apparent removal decreased markedly with increasing temperature, and the Arrhenius analysis yielded an apparent Ea of 30.38 kJ mol^{-1}.

Thermal regeneration at 500 °C for 1 h restored most of the treatment performance: apparent removal decreased from approximately 97% for fresh material to 91% after four reuse cycles, corresponding to about 93.8% retention of the fresh-cycle performance. The combined characterization and adsorption results are consistent with a reusable, thermally robust sepiolite platform in which noncovalent surface interactions and mass-transfer processes contribute to uptake.

The study should be interpreted as treatment of a multicomponent commercial herbicide formulation rather than selective removal of molecular OXY. Specific component-based chromatographic analysis and characterization of the thermal off-gas are essential to determine the fate of OXY, aromatic hydrocarbons from petroleum and other co-formulants. In this context, the results will serve as a solid foundation for further analysis in natural water samples and optimization of the regeneration process at 500 °C.

References

1. Li, L., et al., *Occurrence, ecological risk, and advanced removal methods of herbicides in waters: a timely review.* Environmental Science and Pollution Research, 2024. **31**(3): p. 3297-3319.
2. Li, J., et al., *Contamination remediation and risk assessment of four typical long-residual herbicides: A timely review.* Science of The Total Environment, 2025. **997**: p. 180169.
3. Mohd Ghazi, R., et al., *Health effects of herbicides and its current removal strategies.* Bioengineered, 2023. **14**(1): p. 2259526.
4. Farah, I.F., et al., *Pesticides in aquatic environment: occurrence, ecological implications and legal framework.* Journal of Environmental Chemical Engineering, 2024. **12**(5): p. 114072.
5. Alsa'di, A., N. Mahmoud, and I.A. Al-Khatib, *Utilization of treated municipal effluent for irrigating agricultural land in Palestine: The driving factors and existing practices.* Environmental Research, 2024. **242**: p. 117578.
6. Vaz, T., M.M. Quina, R.C. Martins, and J. Gomes, *Olive mill wastewater treatment strategies to obtain quality water for irrigation: A review.* Science of the Total Environment, 2024. **931**: p. 172676.
7. Székács, A., *Herbicide mode of action*, in *Herbicides*. 2021, Elsevier. p. 41-86.
8. Barker, A.L., et al., *Discovery, mode of action, resistance mechanisms, and plan of action for sustainable use of Group 14 herbicides.* Weed Science, 2023. **71**(3): p. 173-188.
9. Bonnar, D.J. and R.S. Tjeerdema, *Environmental fate and aquatic risk assessment of oxyfluorfen in California rice fields.* Integrated Environmental Assessment and Management, 2025. **21**(1): p. 172-183.
10. Mantzos, N., et al., *Persistence of oxyfluorfen in soil, runoff water, sediment and plants of a sunflower cultivation.* Science of the total environment, 2014. **472**: p. 767-777.
11. Rout, P.R., T.C. Zhang, P. Bhunia, and R.Y. Surampalli, *Treatment technologies for emerging contaminants in wastewater treatment plants: A review.* Science of the Total Environment, 2021. **753**: p. 141990.
12. Crini, G. and E. Lichtfouse, *Advantages and disadvantages of techniques used for wastewater treatment.* Environmental chemistry letters, 2019. **17**(1): p. 145-155.
13. Deng, Y. and R. Zhao, *Advanced oxidation processes (AOPs) in wastewater treatment.* Current pollution reports, 2015. **1**(3): p. 167-176.
14. Chong, M.N., B. Jin, C.W. Chow, and C. Saint, *Recent developments in photocatalytic water treatment technology: a review.* Water research, 2010. **44**(10): p. 2997-3027.
15. Ali, I., *New generation adsorbents for water treatment.* Chemical reviews, 2012. **112**(10): p. 5073-5091.
16. Ewis, D., M.M. Ba-Abbad, A. Benamor, and M.H. El-Naas, *Adsorption of organic water pollutants by clays and clay minerals composites: A comprehensive review.* Applied Clay Science, 2022. **229**: p. 106686.
17. Zyoud, A.H., S.H. Zyoud, and A. Amireh, *An innovative and sustainable approach for water purification: thermal decomposition of tetracycline contaminant adsorbed on thermally stable montmorillonite.* Case Studies in Chemical and Environmental Engineering, 2024. **9**: p. 100631.
18. Dawood, I., et al., *Sustainable water purification through the adsorptive removal of tetracycline via modified clay and regeneration via controlled thermolysis: a reusable and environmentally friendly approach for contaminant mitigation.* Applied Water Science, 2025. **15**(8): p. 215.
19. Salman, S., et al., *Novel water purification technique using kaolinite clay: adsorption followed by thermolysis for complete degradation of methyl orange, reusability, and sustainability.* Discover Applied Sciences, 2025. **7**(7): p. 766.
20. Zyoud, A.H., et al., *Reusable thermally modified natural clay for phenazopyridine removal via adsorption–thermolysis regeneration.* Applied Water Science, 2026.
21. Dawood, I., et al., *Sustainable water treatment using thermally stable natural clay: dual adsorption–thermolysis approach for organic pollutants and nitrate removal.* Scientific Reports, 2025. **15**(1): p. 29888.
22. Amireh, A., et al., *Reusable heat-treated montmorillonite for sustainable phenazopyridine removal from water via adsorption thermolysis regeneration with mechanistic insight.* Discover Applied Sciences, 2026.

23. Madi, S., et al., *Thermally regenerable montmorillonite/sand composite for the adsorptive removal of phenazopyridine from aqueous solutions.* RSC advances, 2026. **16**(39): p. 44832-44851.
24. Ruiz, A.I., C. Ruiz-García, and E. Ruiz-Hitzky, *From old to new inorganic materials for advanced applications: The paradigmatic example of the sepiolite clay mineral.* Applied Clay Science, 2023. **235**: p. 106874.
25. Song, N., A. Hursthouse, I. McLellan, and Z. Wang, *Treatment of environmental contamination using sepiolite: current approaches and future potential.* Environmental Geochemistry and Health, 2021. **43**(7): p. 2679-2697.
26. Ruiz-Hitzky, E., *Molecular access to intracrystalline tunnels of sepiolite.* Journal of Materials Chemistry, 2001. **11**(1): p. 86-91.
27. Suárez, M., J. García-Rivas, E. García-Romero, and N. Jara, *Mineralogical characterisation and surface properties of sepiolite from Polatli (Turkey).* Applied Clay Science, 2016. **131**: p. 124-130.
28. Largo, F., et al., *Design of organically modified sepiolite and its use as adsorbent for hazardous Malachite Green dye removal from water.* Water, Air, & Soil Pollution, 2023. **234**(3): p. 183.
29. Tang, Y., et al., *Modified sepiolite nanoclays in advanced composites for engineering applications.* ACS Applied Nano Materials, 2024. **7**(16): p. 19221-19232.
30. Foo, K.Y. and B.H. Hameed, *Insights into the modeling of adsorption isotherm systems.* Chemical engineering journal, 2010. **156**(1): p. 2-10.
31. Revellame, E.D., et al., *Adsorption kinetic modeling using pseudo-first order and pseudo-second order rate laws: A review.* Cleaner Engineering and Technology, 2020. **1**: p. 100032.
32. Wang, J. and X. Guo, *Adsorption kinetic models: Physical meanings, applications, and solving methods.* Journal of Hazardous materials, 2020. **390**: p. 122156.